X-RAY DIFFRACTION VERIFICATION OF AVIRIS CLAY MINERAL IDENTIFICATION, SUMMITVILLE AREA, SOUTHWESTERN COLORADO

W. S. Duncan[1], E.B. Ledger[1], and V. S. Whitehead[2]
[1]Dept of Geology, SFASU, Nacogdoches, TX
[2] Dept of Forestry, SFASU, Nacogdoches, TX

OBJECTIVES AND INTRODUCTION

The eastern San Juan Mountains of southwestern Colorado are the site of mid- and late-Tertiary volcanic activity. The volcanic activity had two effects on the state of Colorado. Some of the eruptions were extremely large, and magmas formed thick geologic rock units that contributed to the scenic nature of the area. The other effect was that magmas brought precious metals to the earth's near surface that could be exploited by mining.

In the last ten or twenty million years after most of the activity ended, the volcanic bedrock underwent extensive erosion due to the high relief, and chemical weathering of the volcanic rock produced clay minerals in the soil. The original mineralization also emplaced sulfide minerals (mostly non-ore minerals called gangue) that reacted to form very acidic conditions due to sulfide-to-sulfate reactions.

The clay minerals that form in such an environment depend on time (duration) of chemical reactions forming the clays, the parent volcanic rock composition and texture, and the present weathering conditions, including pH. Clay minerals are natural aluminosilicates that form at the earth's surface in response to chemical alteration of higher temperature minerals such as feldspars and mica. Feldspars and mica are K, Na, and Ca aluminosilicates that can form from magmas. They do not form at ambient temperatures, but rather alter to clay.

Analysis of clay minerals is not easy, because they are layer aluminosilicates that can change their structures (d-spacings) in response to their chemical environment, sometimes in a matter of seconds. Standard techniques have been developed over the last eighty or so years to identify various clay minerals using X-ray diffraction (XRD). Even with diagnostic chemical preparation in the controlled environment of the laboratory, clay minerals sometimes require elaborate means to get an unambiguous identification using XRD. A non-laboratory method of clay mineral identification is claimed by a group at the United States Geological Survey (USGS) that uses analysis of visible and near-infrared (NIR) spectra reflected from the ground, and detected from an airplane flying over the area of interest.

The purpose of this study is to analyze by traditional means claims regarding clay mineral identification using the AVIRIS system. A specific study of clay mineral interpretations was conducted on an image of the Summitville mine site in southwestern Colorado (Clark *et al.* 1995). This study centers on verifying clay mineral identifications made by Clark *et al.* (1995).

Most clay mineral structures were originally determined in the 1930s using XRD. This method was developed and applied to minerals by Nobel laureate Linus Pauling. We used XRD to analyze the mineral constituents in the area interpreted by Clark *et al.* (1995). The characterization of clay minerals as distinct crystalline materials as opposed to amorphous material was not proven until XRD was used to verify this in the 1930s. Since then XRD has remained the standard method of clay mineral identification. The objective of this study was to use XRD to attempt to verify a new method, imaging spectroscopy.

Clay Mineralogy

Clay minerals are hydrous aluminosilicates that have a layered structure, and are therefore classified as phyllosilicates. The layers are made of two modular units, tetrahedral and octahedral sheets. In the tetrahedral sheet the dominate cation is Si^{4+}, but Al^{3+} frequently substitutes for Si^{4+}, and Fe^{3+} substitutes occasionally. The chemical formula for all tetrahedral sheets can be represented as T_2O_5 where T represents the cation and O oxygen. Tetrahedral coordination is an atomic arrangement in which an ion is surrounded by four ions of opposite sign. The centers of the surrounding ions form the points of the tetrahedron around the central ion. In the case of clays, Si^{4+} or Al^{3+} and sometimes Fe^{3+}, are the central ions surrounded by O^{2-} ions. The tetrahedral sheets form as a result of individual tetrahedra resting on a tetrahedral face and sharing the oxygen on the three corners with three other tetrahedra. The fourth oxygen points upward, normal to the face on which the tetrahedron is resting and is referred to as the apical oxygen. The sheets that result from this repeated ordered arrangement are called tetrahedral sheets.

The octahedral sheet is a sheet of edge-linked octahedra, unlike the corner linked tetrahedra. The sheets are formed by two planes of closest-packed oxygen ions or hydroxyl ions, with cations occupying the resulting octahedral sites between the two planes. When the centers of six oxygen ions packed around an octahedral cation site are connected, an octahedron forms. When each of these octahedron connects to neighboring oxygen ions, an edge-linked sheet of octahedra forms.

Clay mineral structure is the result of linking these two modular units. The oxygen-to-oxygen or hydroxyl-to-hydroxyl ionic dimensions are approximately the same for the tetrahedral and octahedral sheets. This allows the apical oxygen of the tetrahedral sheets to replace two of the three hydroxyl ions in the octahedral sheet, thus linking the two. This assemblage of one tetrahedral sheet and one octahedral sheet is called a 1:1 layer silicate structure. When another tetrahedral sheet is inverted and placed on top of the 1:1 structure, a 2:1 layer silicate is formed. Because the sheets rarely fit neatly, distortions occur. Such distortions, and the cation/anion replacements that cause these distortions to the structure, give rise to the variety of distinct clay minerals or polytypes, all based on the 1:1 or 2:1 structures.

Weathering in volcanic environments, such as the San Juan Volcanic Field, tend to progress faster than in other environments. Factors such as the abundance of amorphous materials facilitate hydrolysis, and the presence of porous rocks such as pyroclastics enhance leaching and drainage. This rapid weathering can produce azonal distribution of clay minerals.

The clay minerals identified by remote sensing near the Summitville mine site include halloysite or a kaolinite-smectite mixture (Clark *et al.*, 1995). In general, these three minerals can be described as follows: Kaolinite has an assemblage of one tetrahedral sheet and one octahedral sheet and is a 1:1 layer silicate structure or layer type. It is a hydrous aluminosilicate with the chemical formula $Al_4Si_4O_{10}(OH)_8$. Kaolinite is one of the most widespread aluminosilicate minerals, forming as either a residual weathering product, or sometimes by hydrothermal alteration of other aluminosilicates, especially feldspars. Halloysite is a kaolin mineral, and like kaolinite, it has a single layer structure. The primary structural difference between kaolinite and halloysite is the habit. Halloysite has a fibrous habit instead of a platey habit. The smectites include all minerals formerly classified in the montmorillonite group of expansible layer silicates. Smectites have an octahedral sheet in coordination with two tetrahedral sheets in which oxygen atoms are shared. Cationic substitution occurs in the octahedral and tetrahedral sheets, and the corresponding differences in properties and chemical composition are used to classify the smectites (Dixon, 1977).

The formation of halloysite and kaolinite at low temperatures, and how they may be associated is discussed by Dixon (1977). A possible mechanism for the formation of halloysite is platey kaolinite rolling once interlayer hydrogen bonding has been weakened by hydration, thus forming halloysite (Singh and Mackinnon, 1996). Halloysite that formed as the result of the hydration of kaolinite would be occurring with kaolinite.

Fortunately, each of these three individual clay groups, as well as mixed layered clay minerals, can be distinguished by XRD. Both kaolinite and halloysite are single layer structures that yield strong reflections (Table 1). Heating kaolinite at 550 °C for one hour causes it to become amorphous, eliminating its diffraction pattern.

Because of the fibrous habit of halloysite, crystals are not oriented in basal parallel fashion. This results in weak 00l reflections that are generally broad, compared to those of kaolinite, and strong nonbasal reflection between 20 - 30° 2θ. As a result halloysite has a diffraction pattern with a broad 00l and strong asymmetrical hk reflections. Smectites, such as montmorillonite, can be distinguished by their d-spacing reflections (Table 1). Randomly interstratified kaolinite/smectite mixtures are easily distinguished. Air dried samples will yield a peak of d = 7.4 - 8.3Å depending on the kaolinite/smectite ratio. When heat treated to 550° C the kaolinite becomes amorphous and its d-spacing will disappear. Collapsing the structure pulls in the mixed-layered reflection to a lower angle, larger d-spacing (Moore and Reynolds, 1989).

TABLE 1

Mineral	d-spacing	2θ
Kaolinite	7.1Å (001)and 3.57Å (020)	12.47° and 24.94°
Halloysite	10Å (001) and 7.4Å (001)	8.84° and 12.47°
Montmorillonite (Mg saturated)	17.6Å (001)	5.02°

The spectral signatures of the three individual clay groups can also be distinguished provided variations in the clay mineral spectral data are factored into interpretations. The spectral bands are related to the OH^- part of the crystalline structure of these minerals. These band frequencies consist of the sum of OH^- stretching and bending effects (Clark *et al.*, 1990) representing specific resonant bonds in a crystal structure, such as Al-OH bonding. The frequency of the bands varies as cation substitutions in the structure vary because different cation radii change bond lengths and alter the structural geometry (Post and Noble, 1993).

In addition to differences due to cation substitutions, properties of the individual clay minerals, such as the interaction of molecular water with smectites, will effect spectral signatures. Spectral absorptions due to molecular water in montmorillonite are influenced by both the interlayer cation and the moisture environment. Since the absorptions near 1.4 μm and 1.9 μm are composed of multiple, overlapping molecular water features, the band shape, the individual minima, and the band strengths are all important in laboratory spectral analysis and remote sensing of smectites (Bishop *et al.*, 1994).

The NIR Al-OH band position of dioctahedral smectites, muscovite, and other micas appears to be a linear function of Al content (Fig. 1). As the band frequency increases, the unit cell size decreases resulting in varied lower band frequencies (Post and Noble, 1993). Muscovite and kaolinite have NIR band positions that are close to each other, and because of chemical and structural similarities between kaolinite and halloysite it is possible that halloysite could lie in the same range of NIR band positions.

The limitation is in the fact that an interstratified mineral cannot be distinguished from a mixture of minerals. This limitation is evident since infrared spectroscopy probes short-range ordering (Srasra *et al.*, 1994). XRD can penetrate clay minerals enough to be used in distinguishing mixed-layered clay minerals, such as an ordered repeating sequence of kaolinite and montmorillonite, or an unordered repeating sequence as opposed to a mixture of kaolinite and montmorillonite crystals. It is possible that the short-range ordering limitation of NIR spectroscopy may also apply to the ability of the system to distinguish crystalline clay minerals from amorphous material.

GEOLOGIC SETTING

A complete explanation of the formation of the San Juan volcanic field has yet to be proposed. There are no other examples of huge stratovolcanoes, like the San Juans, that exist in the midcontinent. By means of stratigraphic field studies and gravimeter method studies, a general geology of the area has been described by Lipman, Steven, and Mehnert.

Volcanic activity began in late Eocene or early Oligocene time, between 40 and 35 Ma. The early rocks are mainly intermediate in composition, such as andesite, rhyodacite, and mafic quartz latite, erupted from many scattered stratovolcanoes. One such, the Summer Coon Volcano, has been dissected by erosion to reveal a highly symmetrical system of radiating dikes around a central intrusive area. The products derived from these volcanoes coalesced into a composite volcanic field covering more than 25,000 km^2 (Mertzman, 1971).

About 30 Ma the character of volcanic activity changed markedly to predominantly pyroclastic eruptions, and large volume quartz latite and rhyolitic ash flows spread widely from many centers. The earliest ash flows came from the Bonanza caldera in the northeast and the nested Platoro and Summitville calderas in the southern part of the San Juan volcanic field. These were erupted from clusters of early stratovolcanoes. Caldera collapse resulting from the ash flow eruptions largely destroyed the upper parts of these volcanoes (Steven and Lipman, 1976).

The sequence began when magma ascended, possibly from a large batholith, explosively along deep ring fractures into the volcano, destroying its edifice and venting as ash flows. Simultaneously, the structural block bounded by the ring fractures, subsided into the magma chamber, and displaced an amount of magma equal to that vented from the chamber. The result was thick intercaldera ash flow facies within the caldera and outflow facies outside (Ivosevic, 1984).

The materials that were airborne during the ash flow phase, were elutriated or density layered in the air. As the denser material fell, it landed on cooler ground to form glass. The next layer fell on top of the obsidian and formed welded tuff. Ash landed on the welded tuff to form an ash tuff.

In most of the calderas in the San Juan volcanic field, a resurgent dome was emplaced in the center of the caldera. Volcanic domes also formed along ring fractures and along intra caldera linear fractures. Often the caldera walls collapsed along rounded or scalloped faults that were subparallel to the ring fractures. Additional caldera subsidence developed a medial graben on the resurgent dome. These domes and the structures within them provided a host environment for mineral emplacement.

About 29 Ma ash flow eruptions began in the western part of the San Juan volcanic field. The first two of the calderas were largely covered and imperfectly understood. The last three formed much like those in the east. These five calderas formed in less than two million years.

As the activity in the western portion was developing, major pyroclastic eruptions began in the central San Juan volcanic field. This phase of development began about 28 Ma. The result was a sequence of eight major ash flow sheets. Caldera subsidence has been identified or inferred at all of the ash flow source areas. Ash flow activity ended in the central San Juan Mountains about 26.5 Ma.

In the early Miocene, about 25 Ma, the character of the erupted material changed from ash flow tuffs to basaltic material and high-silica alkali-rich rhyolite. This change occurred at approximately the same time as the basin and range faulting in the San Luis Valley segment of the Rio Grande trough. The basaltic eruptions continued intermittently until about 5 Ma. The only rhyolitic ash flow tuff, the Sunshine Peak Tuff, which formed during this period of basalt flows, formed about 22.5 Ma. It formed in and around the concurrently developing Lake City caldera, in the western portion of the San Juans (Lipman, 1975).

A total of 15 calderas are now known in the San Juan volcanic field, and indirect evidence suggests that at least two and perhaps three more exist. A major underlying batholith is indicated by a large Bouguer gravity anomaly that underlies the area containing most of the calderas. Sharp gradients at the margins of the anomaly suggest shallow emplacement of the top of the batholith. The change in eruptive material from the early intermediate composition rocks of the widely scattered stratovolcanoes, to the more silicic ash flows, probably took place as the batholith rose and differentiated beneath the central part of the field. As the roofs of the more gas-charged cupolas of the batholith failed, volumes of ash erupted rapidly, and unsupported segments collapsed to form the calderas. The sequential development of these calderas is believed to reflect the progressive emplacement of the different high level plutons of a composite batholith (Steven and Lipman, 1976).

METHODS OF STUDY

Field Methods

Samples were collected on the ground at Alum Creek in the imaged area. The location was identified on the image found in USGS Bulletin 2220, page 17. The scene was correlated with the USGS 7.5 minute Summitville Quadrangle. The area sampled was along Alum Creek, starting about 1.5 km from the confluence or joining of Alum Creek with the Alamosa River, and extending about 1 km downstream toward the Alamosa River. Samples were taken on slopes that were well exposed to aerial reconnaissance and showed little signs of disturbance or weathering, and were collected by scraping the surface of the slopes. About 10 kg total of sample was collected from the area.

Laboratory Methods

The analysis was performed to confirm the presence of certain minerals. Known peaks were used to identify clay minerals from diffractograms. The minerals to be confirmed were those listed as being imaged by the AVIRIS data and interpreted to be present in the USGS Professional Paper 2220, page 17.

The initial run was a box mount of the first sample collected, AC - 1. This was done to act as a control for the prepared samples. All other runs were slurry mounts used to confirm the presence of various clay minerals. Initially, a standard survey procedure was conducted to provide an estimate of the most abundant clay minerals present. Sufficient sample was used to yield 50-100 mg of clay. This 50-100 mg clay sample was dispersed by "vortexing" in pH 10 sodium carbonate solution. Using balanced centrifuge tubes, a "spin down" was run to separate the clay, what is referred to as the "2 μm cut". The turbid supernatant was decanted to another tube, Mg (II) solution was added, and another "spin down" was run. This resulted in a clear supernatant with clays at the bottom of the tube. The clear supernatant was decanted and discarded. Mg (II) solution was added while vortexing and another "spin down" was run. Again the supernatant was discarded and Mg (II) solution was added while vortexing, and another "spin down" was run. Next, 90% acetone in water was added while vortexing, and a "spin down" run, followed by decanting. Then 2 to 3 drops of 10% glycerol in ethanol was added with vortexing. While vortexing, distilled water was added drop by drop when necessary to achieve a slurry of proper viscosity. When the slurry had the proper viscosity, a Pasteur pipette was used to apply the clay slurry onto a clean, labeled petrographic slide. Slides were set aside to air-dry under a tilted watch glass.

The presence of the various clay minerals can be determined by their characteristic peaks that resulted after Mg saturation. Kaolinite at 7.1Å, montmorillonite at 17.6Å, and halloysite at 10Å. To confirm the presence of kaolinite, a sample can be heated at 550 °C for two hours, which causes the kaolinite to become amorphous and eliminates its diffraction pattern. Halloysite can be detected by looking for additional relatively weak nonbasal reflections that are strongest at about 20 to 35° 2θ. The 001 reflections are usually broader than those from kaolinite, and it will also give strong hk reflections despite efforts to achieve good preferred orientation. Further verification for halloysite can be achieved by gentle heating. This results in a peak of 7.1Å, because the 2.9Å layer of water has been driven out of the clay causing it to collapse to 7.1Å from 10Å.

RESULTS OF STUDY

The results, listed as d-spacings of increasing 2θ , are from X-ray diffractograms (Figs. 2-4) of samples acquired from Alum Creek. Those listed are peaks which had intensities significantly greater than background noise and are listed with associated minerals: h - halloysite, k - kaolinite, m - mica, mm - montmorillonite, j - jarosite, and o - orthoclase. Alum Creek Sample One, box mount, yielded peaks at the d-spacings of 9.88Å - (h,m), 7.11Å - (h,k), 5.92Å - (j), 4.98Å - (m), 4.45Å - (h,k), 4.23Å - (o), 3.56Å - (h,k,j), 3.33Å - (m,k,j), 3.07Å - (j), 2.55Å - (h,k,j), 2.37Å - (h,j), 2.28Å - (j,k), 2.12Å - (k), 1.97Å - (m,j), 1.54Å - (m), 1.43Å - (m), and 1.37Å - (m). Alum Creek Sample One slurry mount gently heat treated yielded peaks at the d-spacings of 16.70Å - (mm), 9.99Å - (h,m), 7.16Å - (h,k), 5.72Å - (j), 5.04Å - (m), 3.53Å - (h,k,mm), 3.33Å - (h,m), 3.08Å - (j), 2.86Å - (j), 2.55Å - (h,k,m), 2.38Å - (h,k,mm), 2.28Å (k,j), and 2.00Å - (m,h). Alum Creek Sample One slurry

mount heated at 550° C for two hours yielded peaks at the d-spacings of 10.01Å -(m), 4.99Å - (m), 3.33Å - (m), 2.70Å - (m), 2.51Å - (m), and 1.99Å - (m).

DISCUSSION

X-ray diffraction data on the samples from the Summitville site showed halloysite, kaolinite, mica, and minor montmorillonite. The determination of the halloysite is based on the sample with no heat treatment compared with those that were heat treated. Comparing AC-1 with gently heat treated AC-1 and AC-1 treated for two hours at 550° C, suggested the presence of both halloysite and kaolinite clay minerals as well as mica. The untreated sample, AC-1, yielded a strong peak at 9.9Å and 7.1Å. Both of these peaks, as well as others, suggested the presence of both kaolinite and halloysite. To further investigate this possibility, AC-1 was gently heated for several hours at 107° C. This intensified the 7.1Å peak and diminished the 9.9Å peak. This effect was not fully demonstrated because the sample had been glycerated, which may have inhibited collapsing of halloysite to 7.1Å spacing (Dixon, 1977). When the same sample was heated for two hours at 550° C, all of the peaks associated with kaolinite and halloysite disappeared, due to the mineral becoming amorphous. Furthermore, the 9.9Å peak narrowed to 10.1Å, due to the presence of mica in the sample. The mica and halloysite had formed a composite peak. The conclusion is that both halloysite and kaolinite were present and possibly formed as described by Singh and MacKinnon (1996).

The results indicated the presence of both kaolinite and halloysite and a slight amount of montmorillonite (Fig. 2-4). They also indicated a large amount of mica (Fig. 2-4), a common primary mineral associated with the volcanism. Mixtures of discrete clay minerals can cause interference with the identification of other clay minerals, especially dioctahedral smectite. The strong kaolinite band may overlap montmorillonite bands, and illite bands may overlap beidellite bands. The main band interference, for clays commonly found together, is from a mixture of kaolinite and montmorillonite (smectite) containing considerable Fe in the structure. Furthermore, the mica could easily be incorrectly identified as a clay, specifically kaolinite, according to the correlation of the primary Al-OH NIR combination bands and Al_2O_3 content for muscovite and kaolinite (Post and Noble, 1993). The correlation does not include halloysite which could also fall in the range close to muscovite.

CONCLUSION

The AVIRIS data used to image the Summitville site is available from JPL on 8 mm tape. They were obtained and yielded usable spectra with composite signatures, because of mixed pixels, which are those pixels with the spectra of more than one material. X-ray diffraction data of samples collected on the ground at Alum Creek in the Summitville area had halloysite, kaolinite, montmorillonite, and mica. The mica, which is from the original volcanic rocks, was much more abundant than the clay minerals.

Because clay minerals are difficult to determine, even in the laboratory, they represent the true test of a sensor's ability to distinguish materials. While the USGS group's interpretation of halloysite, kaolinite, and montmorillonite from AVIRIS data is correct, they fail to mention the abundant mica. This is significant because the similar spectra that mica produces can be confused with the spectra produced by clay minerals imaged. The problem still exists as to how the similar spectra of clay minerals and mica are distinguished from each other in composite signatures. Distinctions made between kaolinite and halloysite can possibly be due to the differences in Al-OH concentrations in muscovite and not to unique spectral signatures of clay minerals.

The purpose of this study was to confirm interpretations made of AVIRIS data by XRD. As a result of this study, mineral data has been produced that can be used to further assess the accuracy of AVIRIS. Scene PG03360-1 is an excellent test site in the continuing development of hyperspectral data. The head of the Alamosa River Basin provides a number of challenges to include several different clay minerals mixed with mica, that can be studied to enhance the abilities of AVIRIS. The conclusion of this study is that interpretations of clay minerals in volcanic environments need to be sensitive to the occurrence and resulting interference of mica, as well as properties of each clay mineral.

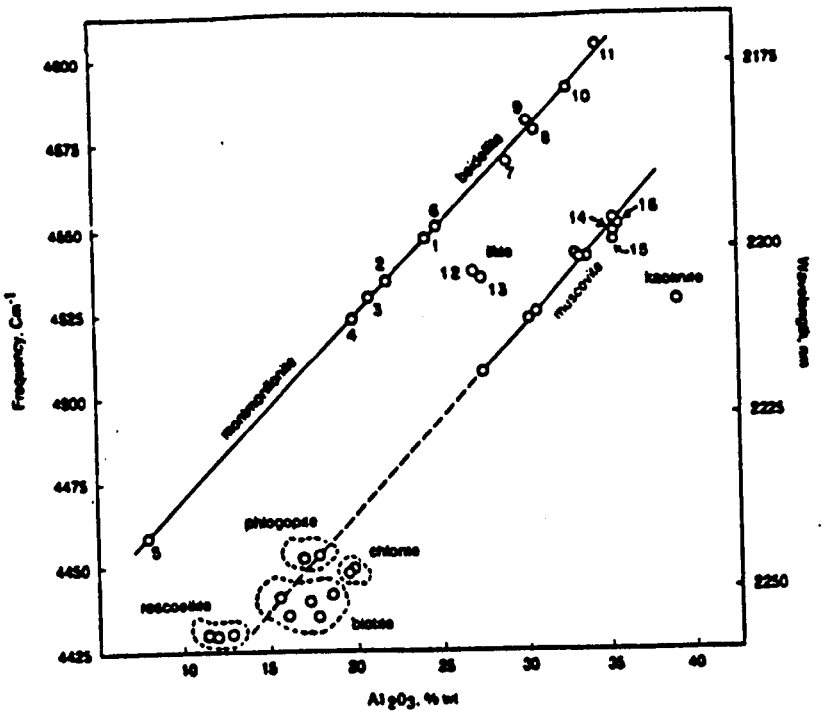

Figure 1. The correlation of the primary Al-OH NIR combination bands and the Al_2O_3 contents for different smectites and illites, plus muscovite, phlogopite, biotite, roscoelite, kaolinite, and chlorite (Post and Noble, 1993).

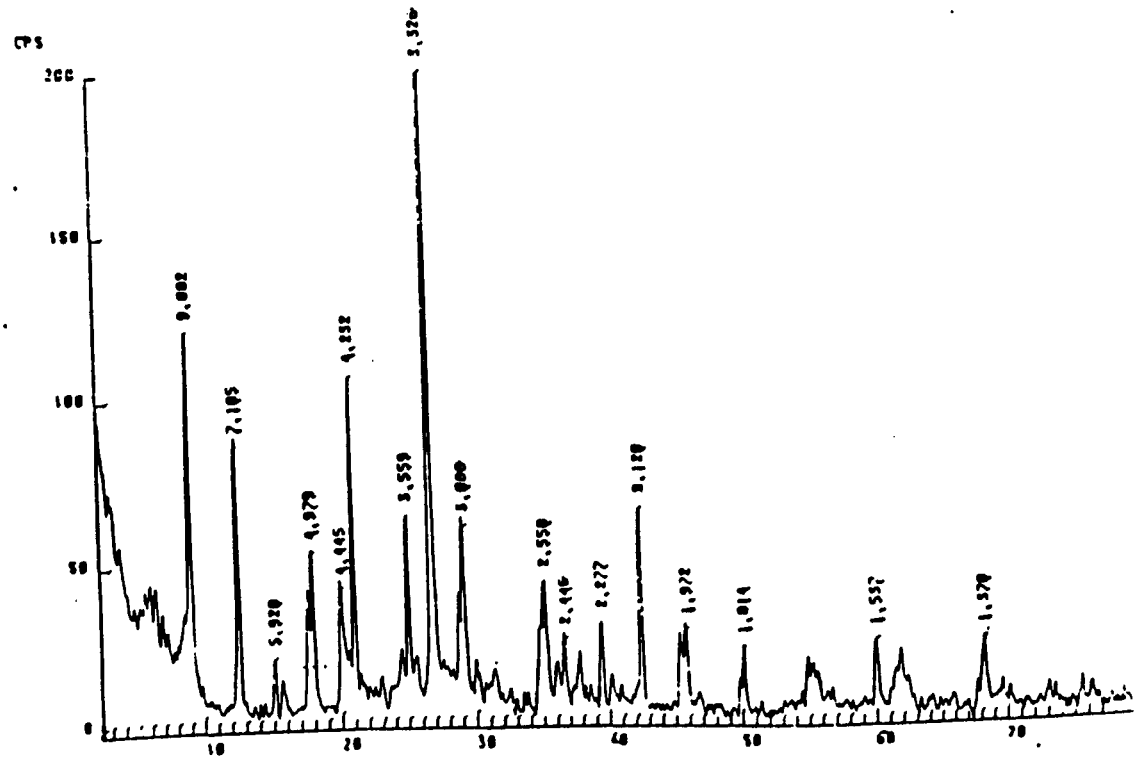

Figure 2. X-ray diffractogram of Alum Creek Sample One, box mount. The X-axis is the 2θ angle from the goniometer and the Y-axis is relative intensity.

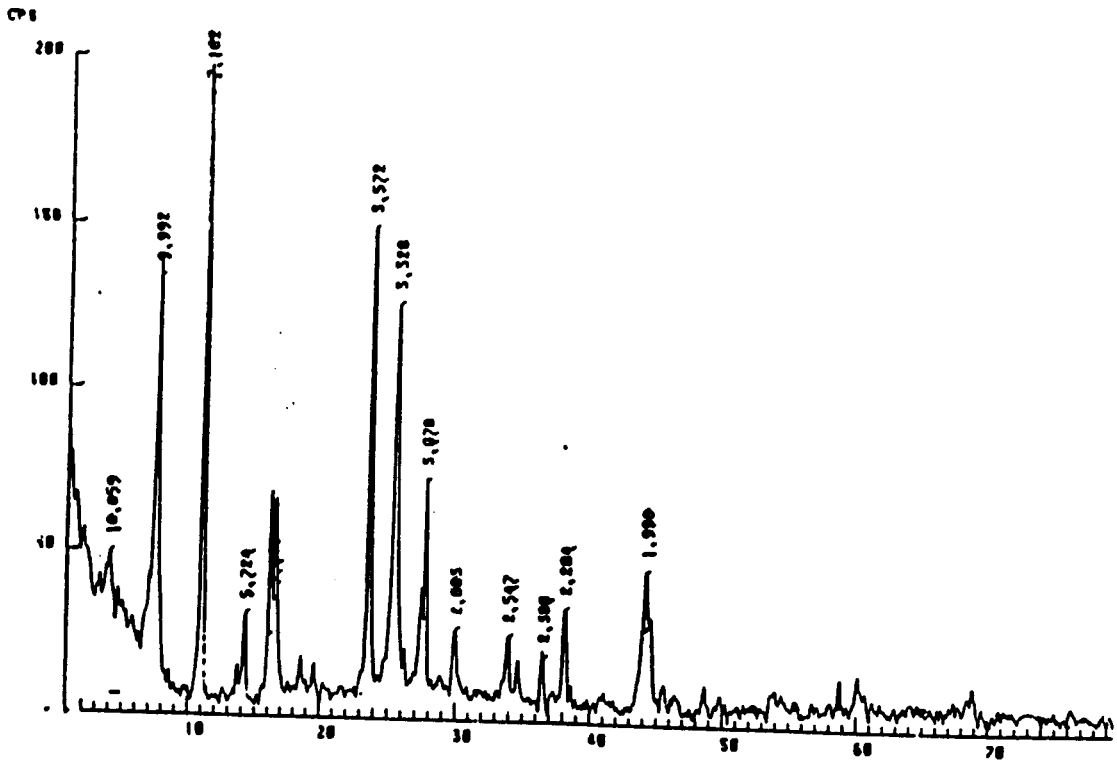

Figure 3. X-ray diffractogram of Alum Creek Sample One, slurry mount, heat treated at 107° C for twelve hours. The X-axis is the 2θ angle from the goniometer and the Y-axis is relative intensity.

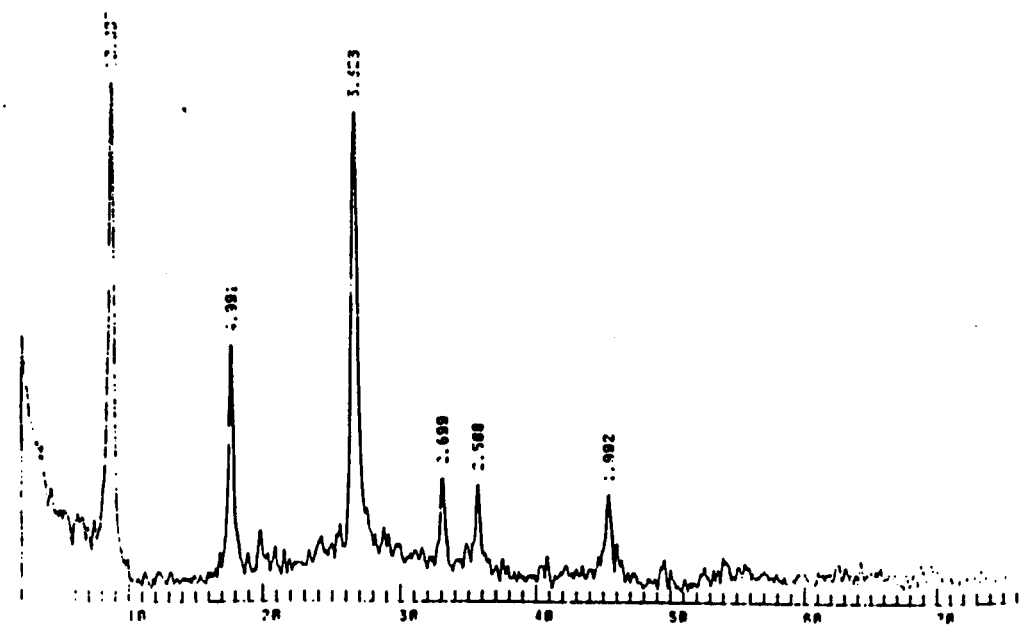

Figure 4. X-ray diffractogram of Alum Creek Sample One, slurry mount, heat treated at 550° C for two hours. The X-axis is the 2θ angle from the goniometer and the Y-axis is relative intensity.

REFERENCES

Bishop, J.L., C.M. Pieters, and J.O. Edwards, 1994, "Infrared Spectroscopic Analyses on the Nature of Water in Montmorillonite", Clays and Clay Minerals, Vol. 42, No. 6, pp. 702-716.

Clark, R.N., T.V.V. King, M. Klejwa, G.A. Swayze, and N. Vergo, 1990, "High Spectral Resolution Reflectance Spectroscopy of Minerals", Jour. Geophys. Research 95, No. 138, 12, 653-12, 680.

Dixon, J.B. and S.B. Weed, 1977, Minerals in Soil Environments, Soil Society of America. Madison, Wisconsin. ch. 9,11.

Ivosevic, S.W., 1984, Gold and Silver Handbook on Geology, Exploration, Economics of Large Tonnage, Low Grade Deposits. Stanley W. Ivosevic, Publisher.

King, T.V.V., 1995, "Environmental Considerations of Active and Abandoned Mine Lands Lessons from Summitville Colorado", U.S. Geol. Survey Bull. 2220, pp.38.

Lipman, P., 1975, "Evolution of the Platoro Caldera and Related Rocks, Southeastern San Juan Mountains, Colorado", U.S. Geol. Survey Prof. Paper 852, pp. 128.

Mertzman Jr., S.A., 1971, "Summer Coon Volcano, Eastern San Juan Mountains, Colorado", New Mexico Geologic Society, pp. 8.

Moore, D.M., and R.C. Reynolds, 1989, X-Ray Diffraction and the Identification and analysis of Clay Minerals. New York: Oxford Press. pp. 179-199.

Post, J.L. and P.N. Noble, 1993, "The Near-Infrared Combination Band Frequencies of Dioctahedral Smectites, Micas, and Illites", Clays and Clay Minerals, Vol. 41, No.6, pp. 639-644.

Singh, B. and I.D.R. MacKinnon , 1996, "Experimental Transformation of Kaolinite to Halloysite", Clays and Clay Minerals, Vol. 44, No. 6, pp. 825-834.

Srasra, E., F. Bergaya, and J.J. Fripiat, 1994, "Infrared Spectroscopic Study of Tetrahedral and Octahedral Substitutions in Interstratified Illite-Smectite Clay", Clays and Clay Minerals, Vol. 42, No. 3, pp. 237-241.

Steven, T.A. and P. Lipman, 1976, "Calderas of the San Juan Volcanic Field, Southwestern Colorado", U.S. Geol. Survey Prof. Paper 958, pp. 35.